



The Effect of Sodium on a Molybdenum Layer by Varying the Growth Pressure on CIGS Solar Absorption Layer

N. J. Suthan Kissinger*

Department of General Studies, Physics Section, Jubail Industrial College, Al Huwayalat, Al Jubail, Eastern Province, Kingdom of Saudi Arabia

Received: 14.12.2023 Accepted: 20.12.2023 Published: 30.12.2023

*suthanjkg@gmail.com

ABSTRACT

Flexible Cu (In, Ga) Se₂ (CIGS) solar cells on stainless-steel (STS) substrates face the problem of efficiency deterioration when iron impurities diffuse into the absorber layer. Iron, the main component of stainless steel, can diffuse through the back contact into the CIGS absorber, where Fe impurities are known to reduce the solar cell performance. In this work, the sodium-doped Molybdenum (Mo-Na) layer was made as a diffusion barrier on STS substrate for various growth pressures. The formed Mo-Na diffusion barrier layer was analyzed by Scanning Electron Microscopy, X-ray diffractometer and UV-Vis Spectrophotometer. X-ray diffraction showed that the films grown on STS substrates had a pure chalcopyrite phase with a preferred (112) orientation Mo back contact and the CIGS layer was subsequently deposited by co-sputtering technique and selenization process, to investigate the Na diffusion through the diffusion barrier into the CIGS absorption layer. The concentrations of Na and Fe diffused in the CIGS layer were also measured by secondary ion mass spectroscopy (SIMS). The SIMS depth profile and optical measurement results demonstrated that the diffusion of Na into the CIGS absorber layer was controlled by varying the working pressure of the Mo-Na layer.

Keywords: Flexible Cu (In, Ga) Se₂ (CIGS); Stainless steel; Sputtering; Diffusion barrier.

1. INTRODUCTION

One of the promising candidates for low-cost, high-efficiency photovoltaic cells is the Cu (In, Ga) Se (CIGS) quaternary compound. These CIGS absorber layers show a much higher absorption coefficient than silicon. CIGS is an established thin film solar cell technology, where conversion efficiencies reached up to 20.4% on the laboratory scale (Reinhard *et al.* 2013). Currently, there are growing demands for solar cell devices on flexible substrates, because of several advantages including good shapeability, lightweight, low material cost, etc. The incorporation of a small amount of sodium (Na) into the p-type absorber layer and its junctions improves the efficiency of the CIGS solar cell significantly (Granata *et al.* 1997). The improvement may be attributed to the higher open circuit voltage (V_{oc}) and fill factor (ff) (Sakurai *et al.* 2003), as well as the higher film conductivity due to an increased carrier density (Kessler *et al.* 2004). However, excessive Na doping degrades cell performance by generating deep defect states that increase the recombination (Su-Huai, *et al.* 1999). In addition, Na is also known to influence the CIGS growth properties.

Many industrial initiatives uplifted the world's solar production to hundreds of megawatts per year, but the material is still far from being understood. There is room for improvement in process control and uniformity,

thereby closing the gap in efficiency between small-area cells and large-area modules from full-scale industrial production (Wallin *et al.* 2012). One of the biggest problems that the industry currently facing is the need for controlling Na diffusion from the substrates to the absorber layer. The influence of Na during the growth of CIGS has been studied by several research groups (Bodegard *et al.* 2000; Rudmann *et al.* 2004; Niles *et al.* 1997; Song *et al.* 2012; Schroeder *et al.* 1997). Na influences the CIGS growth, resulting in some cases, in smaller grains (Ruckh *et al.* 1996) and in some cases, in larger grains and increased texturing of thin films (Nakada *et al.* 2000). There are plenty of suitable flexible metal substrates such as stainless steel (STS), titanium, molybdenum, copper and some alloys that can be used for CIGS solar cells. In particular, STS seems to be an excellent candidate material due to its low cost and high mechanical stability. With the effect of the most promising absorber material CIGS, the certified efficiencies of 18.7% on polyimide (Pianezzi *et al.* 2010) and 17.7% on STS (Jackson *et al.* 2011) foils have been achieved on a lab-scale so far. In comparison to polyimide substrates, the stainless-steel substrates show higher temperature stability and tensile strength, where CIGS process temperatures up to 600 °C can be possible to apply. However, a major disadvantage of stainless steel substrates is that the iron as the main component of stainless steel can diffuse through the back contact into the CIGS absorption layer, where Fe impurities are

known to reduce the solar cell performance (Jackson *et al.* 2004). The main purpose of introducing a diffusion barrier layer in CIGS solar cell module is to reduce the diffusion of impurities from the metal substrate into the solar cells. In particular, to prevent the iron diffusion from STS substrates into the CIGS absorber layers, oxide or nitride diffusion barrier layers are conventionally used. These diffusion barrier layers should have good adhesion to the STS substrates. Indeed, many studies pointed out the role of diffusion barriers and Na on the STS substrate as the impurities blocking layers for the enhancement of solar cell performances (Bjorkman *et al.* 2013; Bae *et al.* 2013; Herz *et al.* 2002). However, these diffusion barriers may increase production costs. The purpose of

this study is to investigate the effect of growth pressure on the diffusion barrier layer on the STS substrate, on the properties of the CIGS-based solar cells.

In this study, the effect of growth pressure on the diffusion barrier layer in the flexible CIGS solar cell in terms of the diffusion of metal ions into the CIGS layers, was investigated (Fig. 1). The Molybdenum-doped Na diffusion barrier layer was simply formed on the STS substrate by annealing the substrate at 600 °C for 1 min under ambient air. The influence and characteristics of the Na concentration diffused from Mo-Na layers were studied by varying the working pressure.

Table 1. Physical properties of the used stainless-steel substrate

Type	Thickness (μm)	R_a (nm)	CTE (ppm K^{-1})	Fe (%)	Cr (%)	Mn (%)	Ni (%)	C (%)	Si (%)
STS 430	126	24.8	10.4	≤ 82	16-18	≤ 1.0	≤ 0.5	≤ 0.12	≤ 1.0

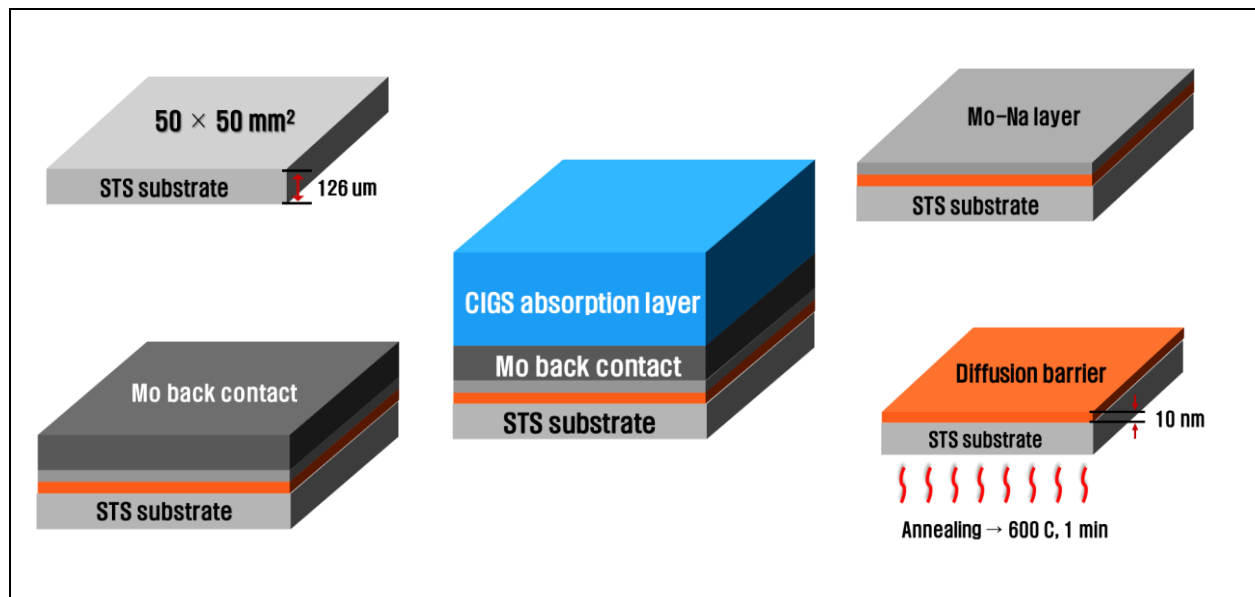


Fig. 1: Schematic representation of different processes involved in the growth of CIGS absorption layer for various growth pressures

2. EXPERIMENTAL PROCEDURE

Commercial stainless steel (STS) substrates of 25 cm² area with a thickness of $d = 126 \mu\text{m}$ were used. Table 1 shows the physical properties of the STS substrates; initially, they were cleaned by ultrasonication in acetone and alcohol for 5 min. The iron oxide ($\alpha\text{-Fe}_2\text{O}_3$) diffusion barrier layer was formed on the STS substrate by annealing at 600 °C for 1 min in the atmosphere.

The annealing time was varied to obtain the suitable thickness of $\alpha\text{-Fe}_2\text{O}_3$ diffusion barrier layers.

Subsequently, the Mo back contact and the CIGS absorption layer were grown by the sputtering process for investigating the diffusion of impurities into the CIGS absorption layer. The Mo back contact layer consisted of a bi-layer structure which was deposited on the $\alpha\text{-Fe}_2\text{O}_3$ diffusion barrier by DC sputtering to obtain an optimal Mo back contact layer. The first layer was deposited at 10 mTorr for better adhesion and the second layer was subsequently deposited at 3 mTorr for a lower resistivity because the adhesion property was improved when the working pressure was higher. Copper-indium-gallium (CIG) layer was then deposited on the Mo back contact by DC magnetron system using a co-sputtering method

with a $\text{Cu}_{0.8}\text{Ga}_{0.2}$ in single targets. In the selenization process, the CIG precursor was selenized by using the thermal evaporation instrument with the effusion cell. The CIG precursor was converted into CIGS on the absorption layer at $500\text{ }^\circ\text{C}$ for an hour to form the p-type CIGS chalcopyrite structure. The schematic representation of the different processes involved is shown in Fig. 1.

The X-ray diffraction (XRD) measurement of the CIGS solar cells was performed by using a Rigaku

diffractometer with $\text{Cu K}\alpha$ radiation. The surface of STS substrate annealed at $600\text{ }^\circ\text{C}$ for 1 min was identified by Raman spectroscopy. The thickness of the diffusion barrier was observed by using Transmission electron microscopy (TEM) analysis. The depth profile was analyzed by secondary ion mass spectroscopy (SIMS) system (CAMECA IMS 7f magnetic sector) with Cs^+ source ions (10 kV, current 30 nA) for Na and Fe diffused from STS substrate.

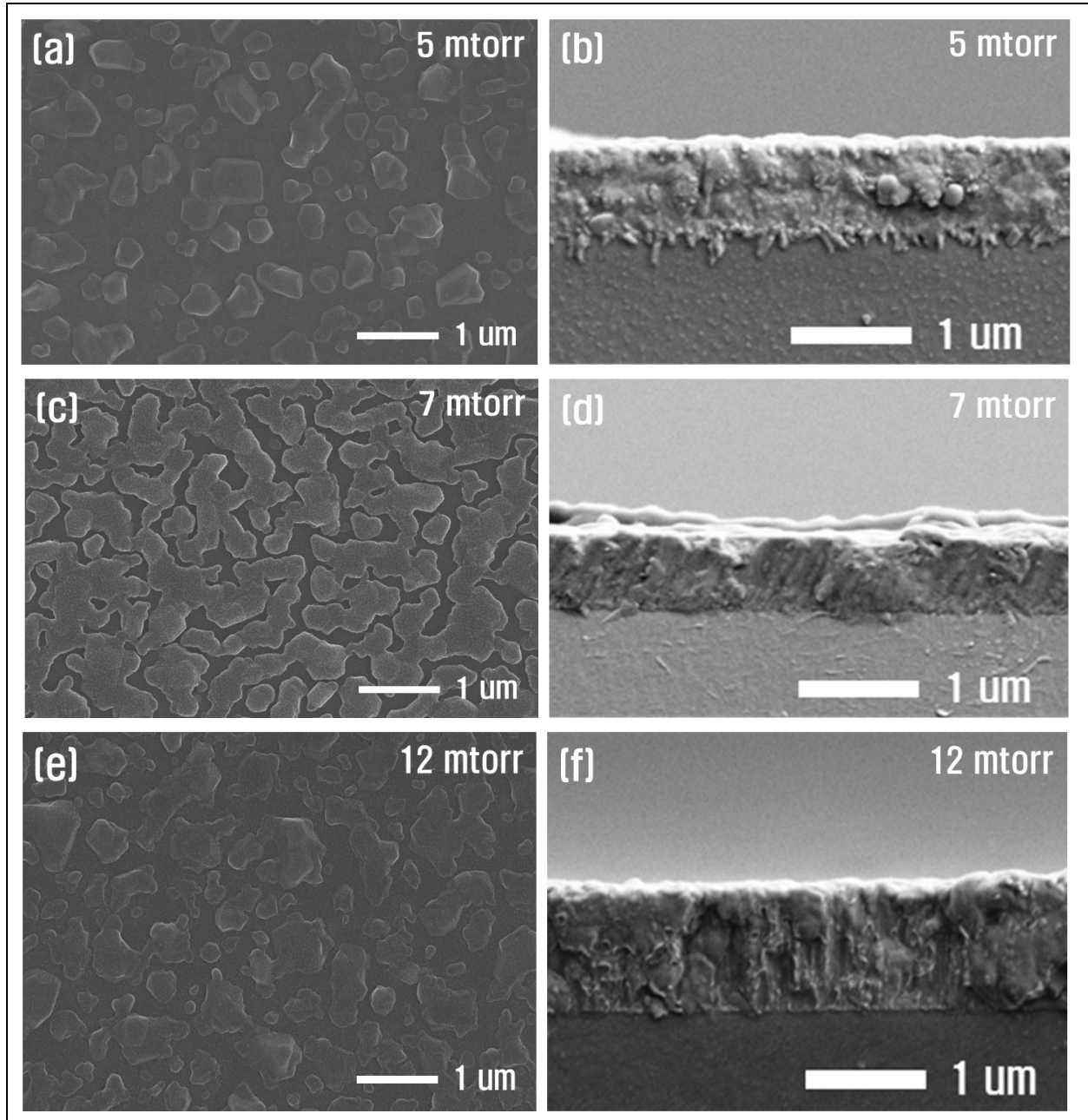


Fig. 2: Plane and Cross-sectional FE-SEM images of Mo-Na layers grown at: (a) & (b) 5 mtorr, (c) & (d) 7 mtorr and (e) & (f) 12 mtorr, respectively

3. RESULTS AND DISCUSSION

3.1 MORPHOLOGY OF Mo-Na LAYER

The surface morphology and cross-section of the Mo-Na layer deposited for different working pressures were characterized by FESEM. Fig. 2 shows the plane and cross-sectional FESEM images of the Mo-Na layer for different working pressures. The cross-sectional view of the sample shows that all the films have columnar grain structure. The films deposited at high pressure are denser with closed grain boundaries while those deposited at low pressure are less dense with more open grain boundaries. The top-view images show larger grain sizes for 12.00 torr compared to the other samples. For pressures higher than 12.00 torr, significantly different grain microstructure was observed due to the high Na content in the layer. A change in grain size for the CIGS absorber layer with high Na concentrations and various Na incorporation methods was also observed by

other research groups (Rudmann *et al.* 2003; Ye *et al.* 2010; Yun *et al.* 2007). The change in the morphology of the Mo-Na layers here indicates that Na is supplied from the Na-doped Mo and its amount is controlled by the various working pressures.

3.2 THE ATOMIC CONCENTRATION ANALYSIS OF Mo-Na SURFACE AND ON THE LAYER

The atomic concentrations on the surface of Mo-Na layer and the Mo-Na layer, shown in Fig. 3, were characterized by EDX measurements. Fig. 3 (a) indicates that the atomic concentration of Na on the surface of the Mo-Na layer was higher than the Mo-Na layer; this in turn indicates that the amount of Na diffused from Mo-Na layer could be controlled by working pressure. It shows that the Na diffusion strongly depends on the microstructure of the Mo-Na layer.

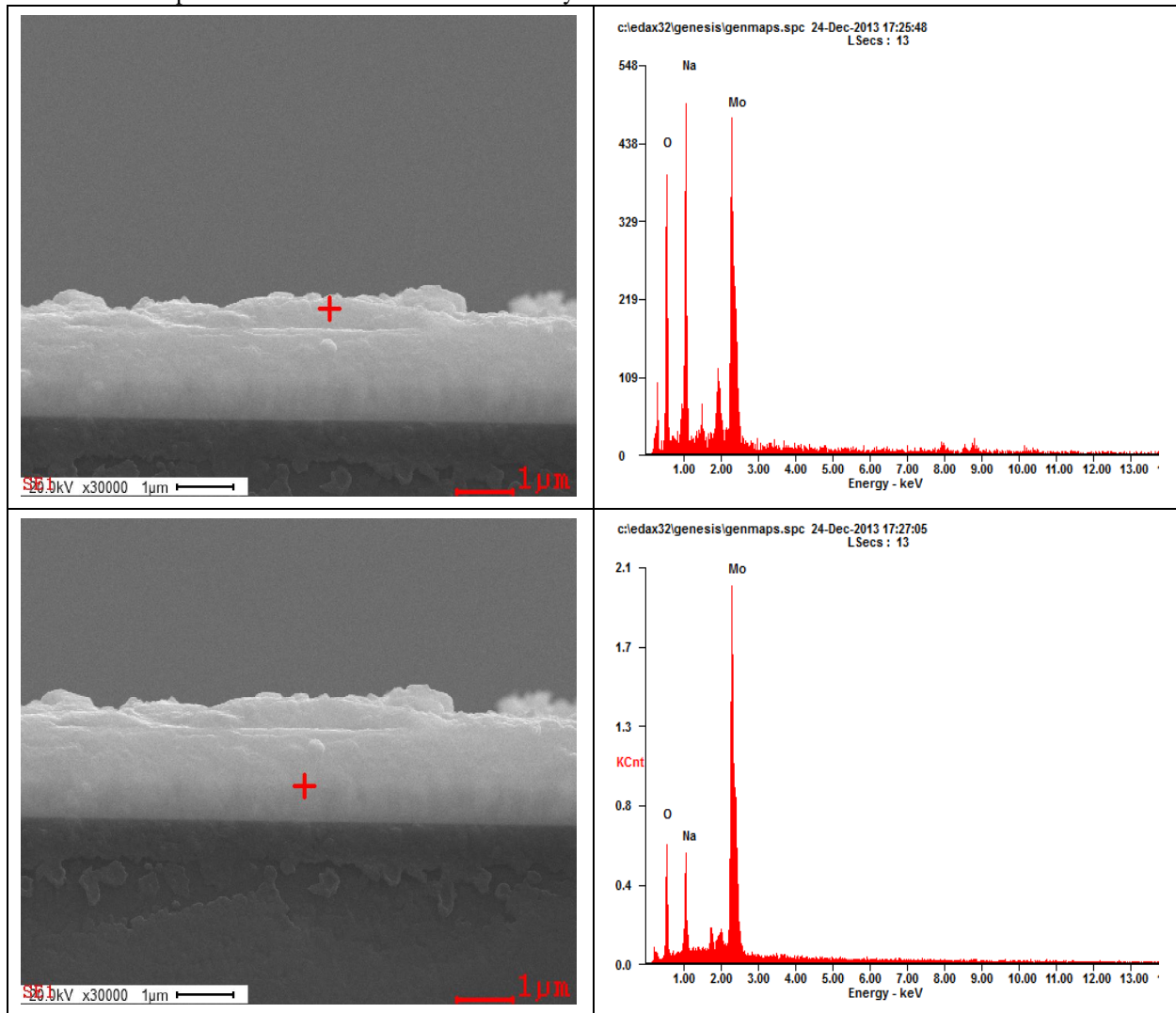


Fig. 3: The atomic concentrations of: (a) Surface on Mo-Na layer and (b) Mo-Na layer, by EDX

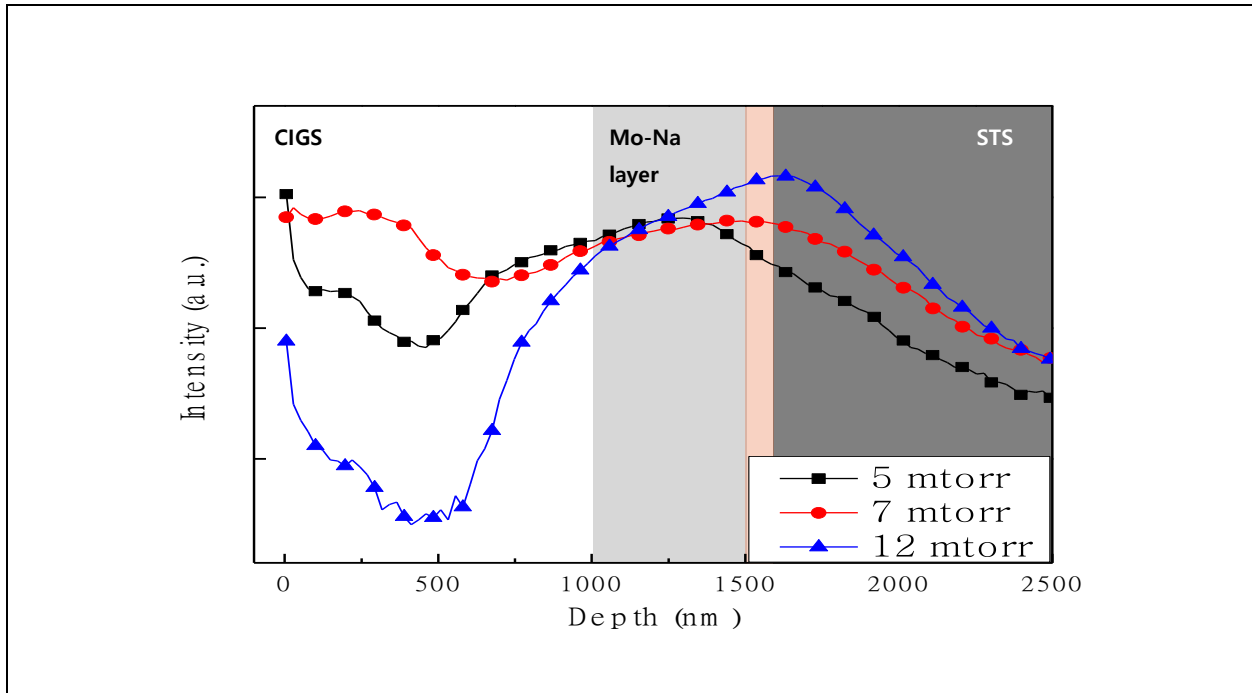


Fig. 4: SIMS depth profile for Na concentration in CIGS absorption layer

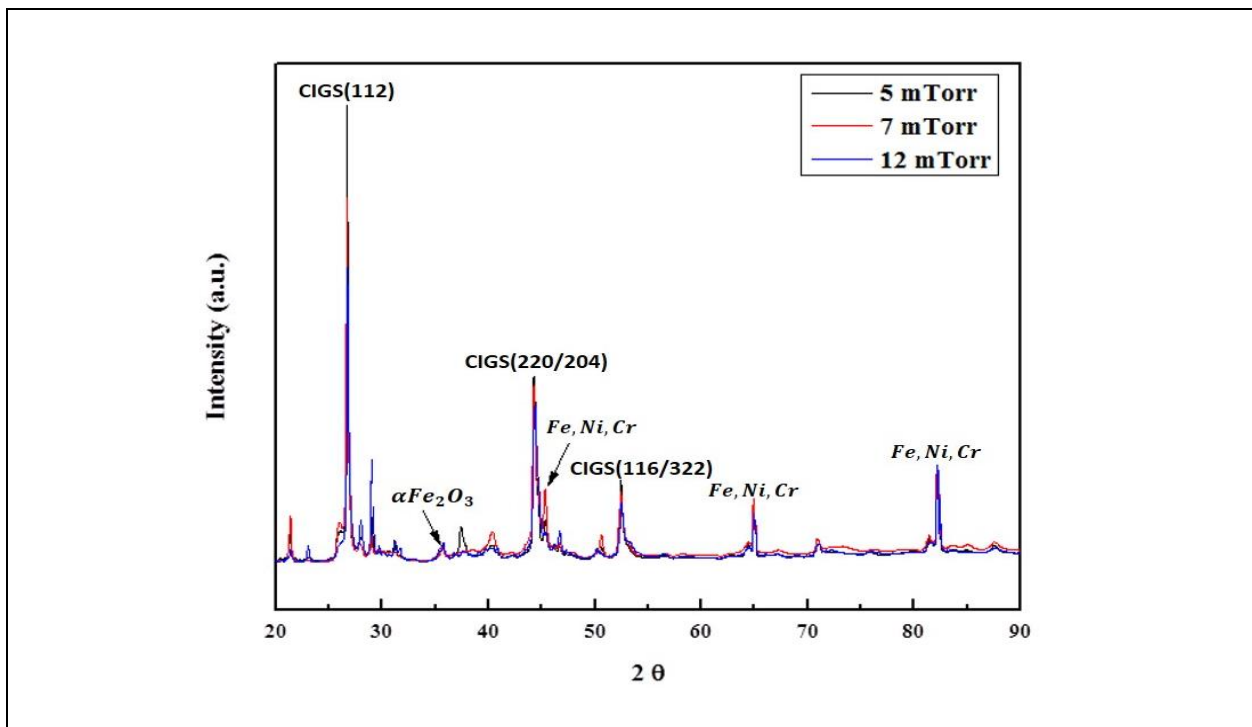


Fig. 5: X-ray diffraction patterns of CIGS absorption layer with various Mo-Na layers

3.3 THE DEPTH PROFILE ANALYSIS

To confirm the existence of Na in the CIGS absorber layers and to verify the dependence of Na diffusion on the Mo-Na layer, a SIMS analysis was performed for different Mo-Na layers prepared by changing the pressures. From the SIMS profile (Fig. 4),

it was clear that Na concentration has a gradient throughout the depth of the sample. The diffusion of doped Na remains fairly even in both horizontal and vertical directions. It was noted that Na is incorporated well into the bulk CIGS absorber layer. The Na and Ga grading was obtained as high intensities and is clearly distinguishable. It was evident that the elements were

richly distributed throughout the thin film and no signs of Se desorption from the surface were observed. This clearly shows that employing the Mo-doped Na layer to supplement sodium by sputtering is an effective and feasible approach, capable of improving sodium distribution and applicable to large areas.

3.4 STRUCTURAL ANALYSIS OF CIGS STRUCTURE

XRD analysis was used to investigate the phase structures of the CIGS solar cell module on the STS substrate. The XRD diffractograms of the CIGS solar cell structure for various growth pressures on the STS substrate are shown in Fig. 5. As shown in the XRD data, the influence of growth pressure on the Na-doped Mo layer was observed. The prominent diffraction peaks corresponding to the CIGS structure were observed at 2θ values of 27, 44 and 53° with respect to (112), (220) and (116/312) planes (JCPDS-#35-1102). All peaks are identified as CIGS chalcopyrite phase with no secondary phase detected. We could also have observed that the (112) peak position exhibits a shift towards higher 2θ values as the working pressure increases. On the other hand, the impurities-related diffraction peaks appeared at

the 2θ values of 44.5 , 65 and 82.5° . When the $\alpha\text{-Fe}_2\text{O}_3$ diffusion barrier layer was introduced in the CIGS solar cell structure, the impurity levels of Fe, Ni and Cr were dramatically reduced. This result showed that the CIGS layer deposited on the Mo-Na layer for various growth pressures on the STS substrate can strongly influence the structural properties of the CIGS solar cell module. It was also observed that the crystallinity of the CIGS absorption layer was improved by varying the growth pressure of the Mo-Na layer. The Mo-Na layer prepared for different growth pressures on the CIGS solar structure can improve the performance of the device.

The mean crystallite size of polycrystalline CIGS thin films can be estimated by Scherrer eq. (Yun *et al.* 2007):

$$D = \frac{K\lambda}{\beta \cos\theta} \quad (1)$$

where, D is the mean crystallite size, λ is the X-ray wavelength ($\lambda = 1.54 \text{ \AA}$ for Cu $K\alpha$ radiation), β is the full-width half-maximum (FWHM), θ is the Bragg angle and K is the shape factor.

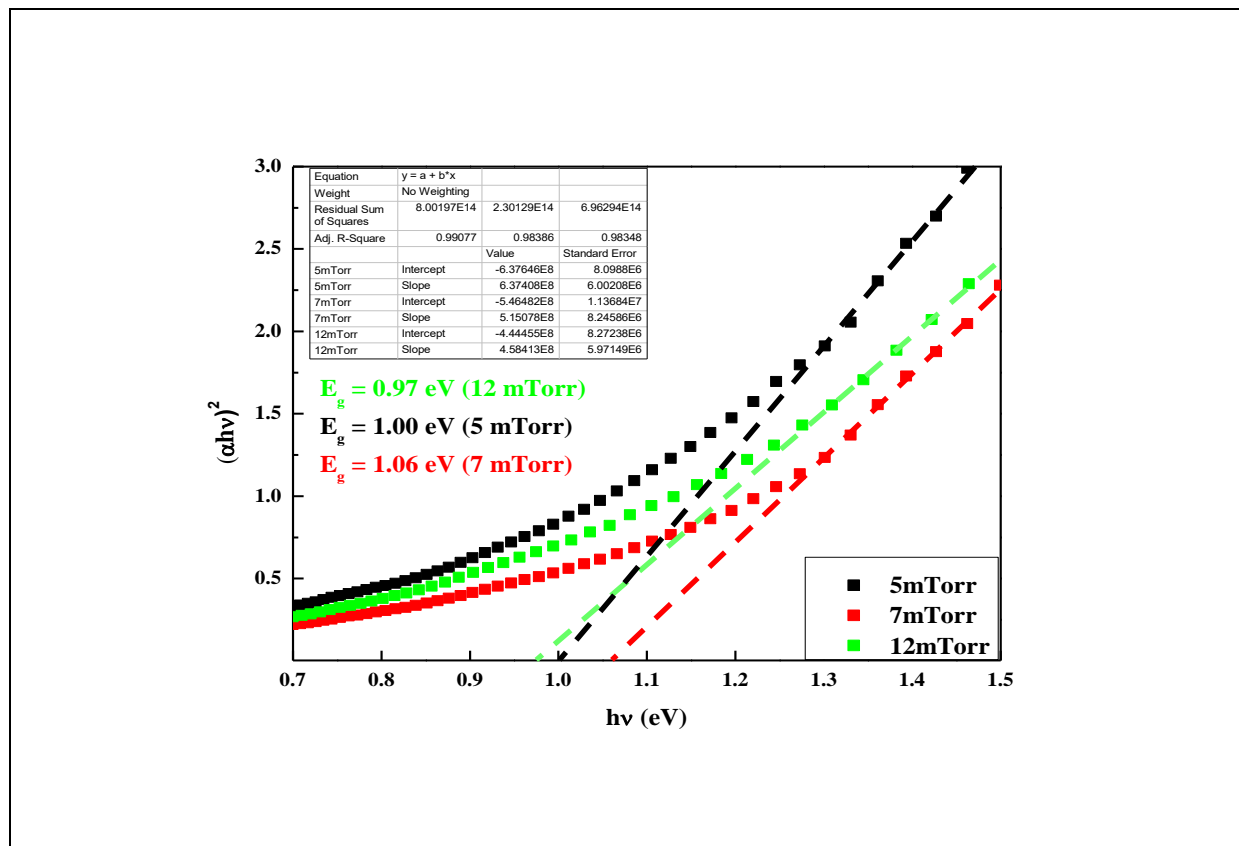


Fig. 6: Optical bandgap of CIGS absorption layer with various Mo-Na layers

3.5 THE BANDGAP STUDIES OF CIGS ABSORPTION LAYER

The dependence of optical bandgap (E_g) on various working pressures was studied using the optical data, including transmittance and reflectance spectra acquired from the CIGS absorption layer on Mo/Mo-Na layer. The optical absorption coefficient (α), was calculated using the following equation (Chuan Chen *et al.* 2013):

$$\alpha = \frac{1}{d} \ln \left[\frac{\sqrt{(1-R)^4 + 4T^2 R^2} + (1-R)^2}{2T} \right] \quad (2)$$

where, d is the film thickness, R is the reflectance and T is the transmittance. Since chalcogenide compounds are direct-gap semiconductors (Yun *et al.* 2007), the following equation can be used (Tauc 1974):

$$\alpha h\nu = A_a (h\nu - E_g)^{1/2} \quad (3)$$

where, A_a is a constant that depends on the transition nature, the effective mass and the refractive index, and $h\nu$ is the incident photon energy. The bandgap was then determined by extrapolating the linear portion of $(\alpha h\nu)^2$ versus $h\nu$ curve to the abscissa; Fig. 6 shows the plot, in the wavelength range of 800 - 1200 nm for the CIGS solar cell structure for different growth pressures. The extrapolation of the tangential line to these plots to zero absorption can provide the appropriate values of the band gap energy of the CIGS solar cell structure with Mo-Na layer. The optical band gap energies of the CIGS solar cell structure for various growth pressures were estimated to be 1.00, 1.06 and 0.97 eV, respectively. It was noted that the bandgap of the CIGS absorption layer was increased by increasing the Na concentration diffused from the Mo-Na layer.

4. CONCLUSION

Sodium diffusion from the substrate is an essential factor in the achievement of high-efficiency CIGS thin-film solar cells. However, controlling the sodium diffusion from soda-lime glass, a well-known and widely used sodium source, is complicated. Moreover, it is necessary to deposit additional sodium source material for CIGS cells with a sodium-free substrate. In this experiment, the effect of the working pressure on the properties of the Mo-Na layer prepared on a stainless steel substrate using an in-line DC magnetron sputtering system was analyzed. The experimental results showed that the working pressure is the important parameter for the high-performance CIGS solar cell module. XRD results confirmed that the films had the right composition and structure with good crystallinity. The microstructure of the Mo-Na layer was identified as a key parameter for

the Na diffusion, where the layer sputtered at high pressure showed enhanced Na out-diffusion performance. The optical bandgap of each film, determined from transmittance and reflectance spectra, increased from 0.97 to 1.06 eV, as the working pressure increased from 5 to 12 mTorr. The results demonstrated that by controlling the growth pressure of Mo-Na layer, it is possible to efficiently incorporate Na into the CIGS absorber layer.

FUNDING

This research received no specific grant from any funding agency in the public, commercial or not-for-profit sectors.

CONFLICTS OF INTEREST

The authors declare that there is no conflict of interest.

COPYRIGHT

This article is an open-access article distributed under the terms and conditions of the Creative Commons Attribution (CC BY) license (<http://creativecommons.org/licenses/by/4.0/>).



REFERENCES

- Bae, D., Kwon, S., Oh, J., Kim, W. K. and Park, H., Investigation of Al₂O₃ diffusion barrier layer fabricated by atomic layer deposition for flexible Cu(In,Ga)Se₂ solar cells, *Renewable Energy*, 55, 62–68 (2013).
<http://dx.doi.org/10.1016/j.renene.2012.12.024>
- Bjorkman, C. P., Jani, S., Westlinder, J., Linnarsson, M., K., Scragg, J. and Edoff, M., Diffusion of Fe and Na in co-evaporated Cu(In,Ga)Se₂ devices on steel substrates, *Thin Solid Films*, 535, 188–192 (2013).
<https://doi.org/10.1016/j.tsf.2012.11.067>
- Bodegard, M., Granath, K. and Stolt, L., Growth of Cu(In,Ga)Se₂ thin films by coevaporation using alkaline precursors, *Thin Solid Films*, 361, 9-16 (2000).
[https://doi.org/10.1016/S0040-6090\(99\)00828-7](https://doi.org/10.1016/S0040-6090(99)00828-7)
- Chuan, C. C., Qi, X., Tsai, M. G., Wu, Y. F., Chen, I. G., Lin, C. Y., Wu, P. H., Chang, K. P., Low-temperature growth of Na doped CIGS films on flexible polymer substrates by pulsed laser ablation from a Na containing target, *Surf. Coat. Technol.*, 231, 209-213 (2013).
<http://dx.doi.org/10.1016/j.surfcoat.2012.06.065>

- Granata, J., E., Sites, J. R., Asher, S. and Matson, R. J., Quantitative incorporation of sodium in CuInSe₂ and Cu(In,Ga)Se₂ photovoltaic devices, *Proceedings of the Conference Record of 26th IEEE Photovoltaic Specialists Conference*, 387-390 (1997). <https://doi.org/10.1109/PVSC.1997.654109>
- Herz, K., Kessler, F., Wachter, R., Powalla, M., Schneider, J., Schulz, A. and Schumacher, U., Dielectric barriers for flexible CIGS solar modules, *Thin Solid Films*, 403-404, 384-389 (2002). [https://doi.org/10.1016/S0040-6090\(01\)01516-4](https://doi.org/10.1016/S0040-6090(01)01516-4)
- Jackson, P., Grabitz, P., Strohm, A., Bilger, G., Schock, H. W., Contamination of Cu (In, Ga)Se₂ solar cells by metallic substrate elements, *Proceedings of the 19th European Photovoltaic Solar Energy Conference*, 1936-1938 (2004).
- Jackson, P., Hariskos, D., Lotter, E., Paetel, S., Wuerz, R., Menner, R., Wischmann, W. and Powalla, M., New world record efficiency for Cu(In,Ga)Se₂ thin-film solar cells beyond 20%, *Prog. Photovoltaics Res. Appl.*, 19(7), 894-897 (2011). <https://doi.org/10.1002/pip.1078>
- Kessler, F. and Rudmann, D., Technological aspects of flexible CIGS solar cells and modules, *Sol. Energy*, 77, 685-695 (2004). <https://doi.org/10.1016/j.solener.2004.04.010>
- Nakada, T., Iga, D., Ohbo, H., Kunioka, A., Effects of sodium on Cu(In,Ga)Se₂-based thin films and solar cells, *Jpn. J. Appl. Phys.*, 361, 9-16 (2000). <https://doi.org/10.1143/JJAP.36.732>
- Niles, D. W., Ramanathan, K., Hasoon, F., Noufi, R., Tielsch, B. J. and Fulghum, J. E., Na impurity chemistry in photovoltaic CIGS thin films: Investigation with x-ray photoelectron spectroscopy, *J. Vacum Sci. Technol. A*, 15, 3044-3049 (1997). <https://doi.org/10.1116/1.580902>
- Pianezzi, F., Chirila, A., Blosch, P., Seyrling, S., Buecheler, S., Kranz, L., Fella, C. and Tiwari, A. N., Electronic properties of Cu(In,Ga)Se₂ solar cells on stainless steel foils without diffusion barrier, *Prog. Photovoltaics Res. Appl.*, 20(3), 253-259 (2012). <https://doi.org/10.1002/pip.1247>
- Reinhard, C. P., Pianezzi, F., Bloesch, P., Uhl, A. R., Fella, C., Kranz, L., Keller, D., Gretener, C., Hagendorfer, H., Jaeger, D., Erni, R., Nishiwaki, S., Buecheler, S. and Tiwari, A. N., Potassium-induced surface modification of Cu(In,Ga)Se₂ thin films for high-efficiency solar cells, *Nat. Mater.*, 12 (12), 1107-1111 (2013). <https://doi.org/10.1038/nmat3789>
- Ruckh, M., Schmid, D., Kaiser, M., Schiffler, R., Walter, T. and Schock, H. W., Influence of substrates on the electrical properties of Cu(In,Ga)Se₂ thin films, *Sol. Energy Mater. Sol. Cells*, 41, 335-434 (1996). [https://doi.org/10.1016/0927-0248\(95\)00105-0](https://doi.org/10.1016/0927-0248(95)00105-0)
- Rudmann, D., Bilger, G., Kaelin, M., Haug, F. J., Zogg, H. and Tiwari, A. N., Effect of NaF coevaporation on structural properties of Cu(In, Ga)Se₂ thin films, *Thin Solid Films*, 431, 37-40 (2003). [https://doi.org/10.1016/S0040-6090\(03\)00246-3](https://doi.org/10.1016/S0040-6090(03)00246-3)
- Rudmann, D., Da, C. A. F., Kaelin, M., Kurdesau, F., Zogg, H., Tiwari, A. N., Bilger, G., Efficiency enhancement of Cu(In,Ga)Se₂ solar cells due to post-deposition Na incorporation, *Appl. Phys. Lett.*, 84(7), 1129-1131 (2004). <https://doi.org/10.1063/1.1646758>
- Sakurai, Y., Yamada, A., Fons, P., Matsubara, K., Kojima, T., Niki, S., Baba, T., Tsuchimochi, T. and Kimura, N. H., Adjusting the sodium diffusion into CuInGaSe₂ absorbers by preheating of Mo/SLG substrates, *J. Phys. Chem. Solids*, 64, 1877-1880 (2003). [https://doi.org/10.1016/S0022-3697\(03\)00173-2](https://doi.org/10.1016/S0022-3697(03)00173-2)
- Schroeder, D. J. and Rockett, A. A., Electronic effects of sodium in epitaxial CuIn_{1-x}Ga_xSe₂, *J. Appl. Phys.*, 82(10), 4982-2985 (1997). <https://doi.org/10.1063/1.366365>
- Song, X., Caballero, R., Felix, R., Gerlach, D. and Kaufmann, C. A., Schock, H. W., Wilks, R. G., Bar, M., Na incorporation into Cu(In,Ga)Se₂ thin-film solar cells absorbers deposited on polyimide: Impact on the chemical and electronic surface structure, *J. Appl. Phys.*, 111(3), 1-9 (2012). <https://doi.org/10.1063/1.3679604>
- Su-Huai, W., Zhang, S. B. and Alex, Z., Effects of Na on the electrical and structural properties of CuInSe₂, *J. Appl. Phys.*, 85, 7214-7218 (1999). <https://doi.org/10.1063/1.370534>
- Tauc, J., Amorphous and Liquid Semiconductors, *Springer*, New York, 97-103 (1974).
- Wallin, E., Malm, U., Jarmar, T., Lundberg, O., Edoff, M. and Stolt, L., World-record Cu(In,Ga)Se₂-based thin-film sub-module with 17.4% efficiency, *Prog. Photovoltaics Res. Appl.*, 20, 851-854 (2012). <https://doi.org/10.1002/pip.2246>
- Ye, S., Tan, X., Jiang, M., Fan, B., Tang, K., Zhuang, S., Impact of different Na-incorporating methods on Cu(In, Ga) Se₂ thin film solar cells with a low-Na structure, *Appl. Opt.*, 49, 1662-1665 (2010). <http://dx.doi.org/10.1364/AO.49.001662>
- Yun, J. H., Kim, K. H., Kim, M., Ahn, B. T., Ahn, S. J., Lee, J. C. and Yoon, K. H., Fabrication of CIGS solar cells with a Na-doped Mo layer on a Na-free substrate, *Thin Solid Films*, 515, 5876-5879 (2007). <https://doi.org/10.1016/j.tsf.2006.12.156>